LETTER

doi:10.1038/nature12569

Slowly fading super-luminous supernovae that are not pair-instability explosions

M. Nicholl[1], S. J. Smartt[1], A. Jerkstrand[1], C. Inserra[1], M. McCrum[1], R. Kotak[1], M. Fraser[1], D. Wright[1], T.-W. Chen[1], K. Smith[1], D. R. Young[1], S. A. Sim[1], S. Valenti[2,3], D. A. Howell[2,3], F. Bresolin[4], R. P. Kudritzki[4], J. L. Tonry[4], M. E. Huber[4], A. Rest[5], A. Pastorello[6], L. Tomasella[6], E. Cappellaro[6], S. Benetti[6], S. Mattila[7,8], E. Kankare[7,8], T. Kangas[8], G. Leloudas[9,10], J. Sollerman[11], F. Taddia[11], E. Berger[12], R. Chornock[12], G. Narayan[12], C. W. Stubbs[12], R. J. Foley[12], R. Lunnan[12], A. Soderberg[12], N. Sanders[12], D. Milisavljevic[12], R. Margutti[12], R. P. Kirshner[12,13], N. Elias-Rosa[14], A. Morales-Garoffolo[14], S. Taubenberger[15], M. T. Botticella[16], S. Gezari[17], Y. Urata[18], S. Rodney[19], A. G. Riess[19], D. Scolnic[19], W. M. Wood-Vasey[20], W. S. Burgett[4], K. Chambers[4], H. A. Flewelling[4], E. A. Magnier[4], N. Kaiser[4], N. Metcalfe[21], J. Morgan[4], P. A. Price[22], W. Sweeney[4] & C. Waters[4]

Super-luminous supernovae[1–4] that radiate more than 10^{44} ergs per second at their peak luminosity have recently been discovered in faint galaxies at redshifts of 0.1–4. Some evolve slowly, resembling models of 'pair-instability' supernovae[5,6]. Such models involve stars with original masses 140–260 times that of the Sun that now have carbon–oxygen cores of 65–130 solar masses. In these stars, the photons that prevent gravitational collapse are converted to electron–positron pairs, causing rapid contraction and thermonuclear explosions. Many solar masses of ^{56}Ni are synthesized; this isotope decays to ^{56}Fe via ^{56}Co, powering bright light curves[7,8]. Such massive progenitors are expected to have formed from metal-poor gas in the early Universe[9]. Recently, supernova 2007bi in a galaxy at redshift 0.127 (about 12 billion years after the Big Bang) with a metallicity one-third that of the Sun was observed to look like a fading pair-instability supernova[1,10]. Here we report observations of two slow-to-fade super-luminous supernovae that show relatively fast rise times and blue colours, which are incompatible with pair-instability models. Their late-time light-curve and spectral similarities to supernova 2007bi call the nature of that event into question. Our early spectra closely resemble typical fast-declining super-luminous supernovae[2,11,12], which are not powered by radioactivity. Modelling our observations with 10–16 solar masses of magnetar-energized[13,14] ejecta demonstrates the possibility of a common explosion mechanism. The lack of unambiguous nearby pair-instability events suggests that their local rate of occurrence is less than 6×10^{-6} times that of the core-collapse rate.

The discovery of a luminous transient, PTF 12dam, was first reported[15] by the Palomar Transient Factory on 23 May 2012. We recovered the transient in Pan-STARRS1 (Panoramic Survey Telescope and Rapid Response System) 3π survey data, between 13 and 29 April 2012, at right ascension (RA) 14 h 24 min 46.21 s and declination (dec.) +46° 13′ 48.66″. We triggered spectroscopic follow-up, beginning with Gran Telescopio Canarias and the William Herschel Telescope (23–25 May 2012). No traces of hydrogen or helium were visible, leading to a type Ic classification, and strong host galaxy lines provided a redshift measurement $z = 0.107$ (ref. 15). A second, similar transient, PS1-11ap, was discovered in the Pan-STARRS1 Medium Deep Survey on 2 January 2011 (RA 10 h 48 min 27.72 s, dec. +57° 09′ 09.2″). Early spectra showed host galaxy emission lines at $z = 0.523$ (for details of the data, see Supplementary Information sections 1–3).

The high luminosity and slow decline of their light curves (Fig. 1, Extended Data Tables 1–3, Extended Data Fig. 1) marked out PTF 12dam and PS1-11ap as potential SN 2007bi-like events: that is, they could be pair-instability supernova (PISN) candidates discovered soon after explosion. SN 2007bi was discovered well after maximum light. Although the peak was recovered in the R band[1], the light-curve rise and early spectra were missed. Because of the long diffusion timescale associated with the very massive ejecta in PISN models, the time to reach maximum light ($\gtrsim 100$ days) is a crucial observational test. The rise time for SN 2007bi was estimated at 77 days (ref. 1), but this was based on a parabolic fit to the data around the peak, and so was not well constrained. Our Pan-STARRS1 images reveal multiple early detections of PTF 12dam and PS1-11ap in g_{P1}, r_{P1} and i_{P1} bands at around 50 and 35 rest-frame days before peak brightness, respectively (Extended Data Fig. 2). PTF 12dam is not detected in z_{P1} images on 1 January 2012, 132 days before the peak. Although their light curves match the declining phases of SN 2007bi and the PISN models quite well, PTF 12dam and PS1-11ap rise to maximum light a factor of ~2 faster than these models.

The spectra of PTF 12dam and PS1-11ap show them to be similar supernovae. After 50 days from the respective light curve peaks, these spectra are almost identical to that of SN 2007bi at the same epoch (Fig. 2, Extended Data Table 4, Extended Data Fig. 3). The blue colours are in stark contrast to the predictions of PISN models[7,8] (Fig. 3, Extended Data Fig. 4), which show much cooler continua below 5,000 Å and marked drop-offs in the ultraviolet. Particularly around and after maximum light, PISN colours are expected to evolve to the red owing to increasing blanketing by iron group elements[7,8] abundant in their ejecta. We see no evidence of line blanketing in our spectra, even down to 2,000 Å (rest frame) in PS1-11ap, which suggests lower iron group abundances and a higher degree of ionization than in PISN models. Such conditions are fulfilled in models of ejecta reheated by magnetars—highly magnetic, rapidly rotating nascent pulsars[13,16,17]. The pressure of the magnetar wind on the inner ejecta can form a dense shell[13,14,17] at near-constant photospheric velocity. For PTF 12dam, the velocities of

[1]Astrophysics Research Centre, School of Mathematics and Physics, Queen's University Belfast, Belfast BT7 1NN, UK. [2]Las Cumbres Observatory Global Telescope Network, 6740 Cortona Drive, Suite 102 Goleta, California 93117, USA. [3]Department of Physics, Broida Hall, University of California, Santa Barbara, California 93106, USA. [4]Institute of Astronomy, University of Hawaii, 2680 Woodlawn Drive, Honolulu, Hawaii 96822, USA. [5]Space Telescope Science Institute, 3700 San Martin Drive, Baltimore, Maryland 21218, USA. [6]INAF, Osservatorio Astronomico di Padova, Vicolo dell'Osservatorio 5, 35122 Padova, Italy. [7]Finnish Centre for Astronomy with ESO (FINCA), University of Turku, Väisäläntie 20, FI-21500 Piikkiö, Finland. [8]Tuorla Observatory, Department of Physics and Astronomy, University of Turku, Väisäläntie 20, FI-21500 Piikkiö, Finland. [9]The Oskar Klein Centre, Department of Physics, Stockholm University, 10691 Stockholm, Sweden. [10]Dark Cosmology Centre, Niels Bohr Institute, University of Copenhagen, 2100 Copenhagen, Denmark. [11]The Oskar Klein Centre, Department of Astronomy, Stockholm University, 10691 Stockholm, Sweden. [12]Harvard-Smithsonian Center for Astrophysics, 60 Garden Street, Cambridge, Massachusetts 02138, USA. [13]Kavli Institute for Theoretical Physics, University of California Santa Barbara, Santa Barbara, California 93106, USA. [14]Institut de Ciències de l'Espai (IEEC-CSIC), Facultat de Ciències, Campus UAB, 08193 Bellaterra, Spain. [15]Max-Planck-Institut für Astrophysik, Karl-Schwarzschild-Strasse 1, 85741 Garching, Germany. [16]INAF–Osservatorio Astronomico di Capodimonte, Salita Moiariello 16, I-80131 Napoli, Italy. [17]Department of Astronomy, University of Maryland, College Park, Maryland 20742-2421, USA. [18]Institute of Astronomy, National Central University, Chung-Li 32054, Taiwan. [19]Department of Physics and Astronomy, Johns Hopkins University, 3400 North Charles Street, Baltimore, Maryland 21218, USA. [20]Pittsburgh Particle Physics, Astrophysics, and Cosmology Center, Department of Physics and Astronomy, University of Pittsburgh, 3941 O'Hara Street, Pittsburgh, Pennsylvania 15260, USA. [21]Department of Physics, Durham University, South Road, Durham DH1 3LE, UK. [22]Department of Astrophysical Sciences, Princeton University, Princeton, New Jersey 08544, USA.

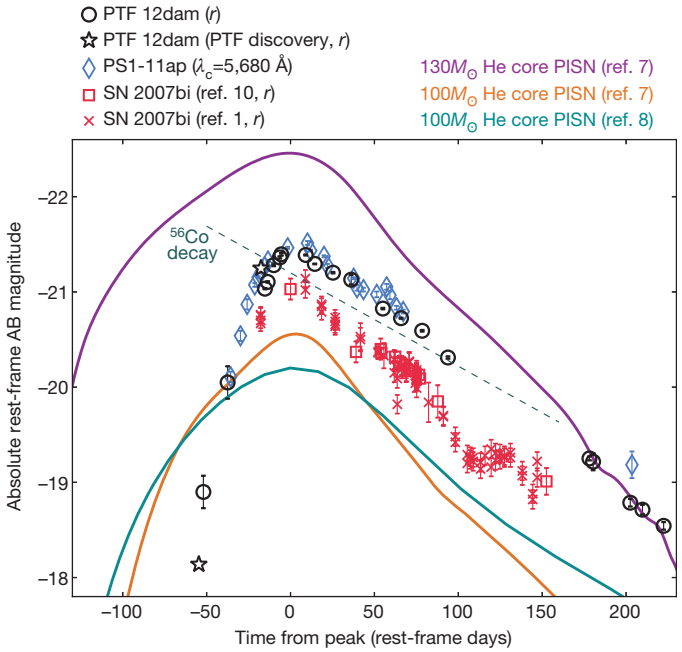

Figure 1 | Optical light curves of slow-fading super-luminous supernovae. Data for PTF 12dam (including discovery data announced[15] by PTF) and SN 2007bi (from refs 1 and 10) are given in the SDSS (Sloan Digital Sky Survey) r band (central wavelength $\lambda_c = 6{,}230$ Å), while for PS1-11ap at $z = 0.523$, the PS1 z_{P1} filter corresponds to a rest-frame filter of $\lambda_c = 5{,}680$ Å (width of passband $\lambda_{width} \approx 1{,}350$ Å), similar to SDSS r. The first three PS1-11ap points were transformed from i_{P1} using the observed $i_{P1} - z_{P1}$ colour (see Supplementary Information sections 2 and 3 for details of the data, including *k*-corrections, colour transformations and extinction). The three supernovae (open symbols) display the same slow decline from maximum, matching the rate expected from ^{56}Co decay (dashed line) with close to full γ-ray trapping (although similar declines can be generated for ~100 days after peak from magnetar spin-down[21]). Powering these high luminosities radioactively requires at least 3–7$M_\odot$ of ^{56}Ni (refs 1, 10, 18 and 20), suggesting an extremely massive progenitor and possible pair-instability explosion[1]. Also shown are synthetic SDSS *r*-band light curves (solid lines) generated from published one-dimensional models[7,8] of PISNs from 100–130$M_\odot$ stripped helium cores. These fit the decline phase well, but do not match our early observations. The rise time of a PISN is necessarily long (rising 2.5 mag to peak in 95–130 days), because heating from ^{56}Ni/^{56}Co decay occurs in the inner regions, and the resultant radiation must then diffuse through the outer ejecta, which typically has mass >80$M_\odot$ (ref. 7). Models with higher-dimensional outward mixing of ^{56}Ni are likely to show even shallower gradients in the rising phase, while as-yet unexplored parameters such as rotation and magnetic fields will have little effect on the diffusion timescale, which is set by the mass, kinetic energy and opacity of the ejecta (see Supplementary Information section 5.2). The pre-peak photometry of PTF 12dam and PS1-11ap shows only a moderately slow rise over 50–60 days, which is therefore physically inconsistent with the PISN models. Error bars, $\pm 1\sigma$.

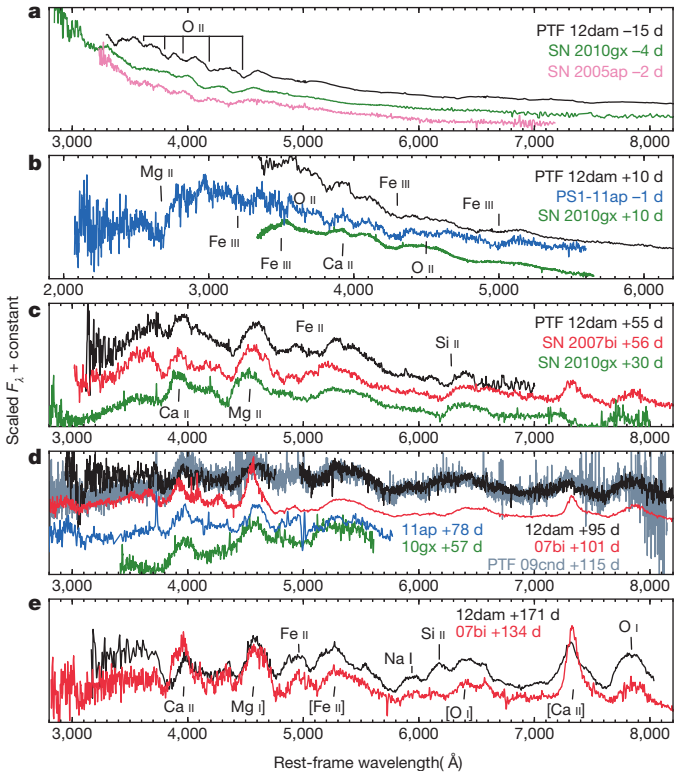

Figure 2 | Spectral evolution of PTF 12dam and PS1-11ap from super-luminous supernovae of type I to SN 2007bi-like. **a**–**e**, We show spectra of PTF 12dam, PS1-11ap, SN 2007bi, and the well-studied superluminous supernovae of type I, SN 2010gx[11], SN 2005ap[2] and PTF09cnd[2]. Our spectra have been corrected for extinction and shifted to respective rest frames (details of reduction and analysis, including construction of model host continua for subtraction from **d** and **e**, in Supplementary Information section 3), and scaled to facilitate comparison. Phases are given in rest-frame days relative to maximum light. No hydrogen or helium are detected at any stage (near-infrared spectra of PTF 12dam, obtained at +13 days and +27 days, also show no He I; see Supplementary Information section 3). **a**, Before and around peak, our objects show the characteristic blue continua and O II absorptions common to super-luminous supernovae of type I/Ic[2,12,21], although the lines in the slowly evolving objects are at lower velocities than are typically seen in those events. **b**, Shortly after peak, Fe III features emerge, along with the Mg II and Ca II lines that dominate superluminous type I supernovae at this phase. **c**, By 55 days after peak, PTF 12dam is almost identical to SN 2007bi. We note that these objects still closely resemble SN 2010gx, but seem to be evolving on longer timescales (consistent with the slower light-curve evolution). **d**, At ~100 days, PTF 12dam also matches PTF09cnd[2], which faded slowly for a superluminous type I supernova after a 50-day rise. **e**, The spectra are now quasi-nebular, dominated by emission lines of Ca II H and K, Mg I] 4,571 Å, Mg I 5,183 Å + [Fe II 5,200] Å blend, [O I] 6,300, 6,364 Å, [Ca II] 7,291, 7,323 Å, and O I 7,774 Å, but some continuum flux is still visible. We find that the emission line intensities can be reproduced by ejecta from a 15$M_\odot$ type I supernova at a few thousand degrees, without requiring a large mass of iron (Supplementary Information section 4).

spectral lines are close to 10,000 km s^{-1} at all times. Intriguingly, the early spectra of our objects are very similar to those of superluminous supernovae of type I (refs 2, 11, 12) and evolve in the same way, but on longer timescales and with lower line velocities (Fig. 2).

Nebular modelling of SN 2007bi spectra has been used to argue[1] for large ejected oxygen and magnesium masses of 8–15$M_\odot$ and 0.07–0.13$M_\odot$, respectively (where $M_\odot$ is the solar mass). Such masses are actually closer to values in massive core-collapse models[18] than in PISN models, which eject ~40$M_\odot$ oxygen and ~4$M_\odot$ magnesium[1,8,9]. In the work reported in ref. 1, an additional 37$M_\odot$ in total of Ne, Si, S, and Ar were added to the model, providing a total ejecta mass consistent with a PISN. However, this was not directly measured[1], because these elements lack any identified lines. These constraints are important, so we investigated line formation in this phase using our own non-local thermodynamic equilibrium code[19] (Extended Data Fig. 5; Supplementary Information section 4). We found that the luminosities of [O I] 6,300, 6,364 Å, O I 7,774 Å and Mg I] 4,571 Å, and the feature at 5,200 Å ([Fe II] + Mg I), can be reproduced with 10–20$M_\odot$ of oxygen-dominated ejecta, containing ~0.001–1$M_\odot$ of iron, given reasonable physical conditions (singly ionized ejecta at a few thousand degrees). Thus, although the nebular modelling of SN 2007bi in ref. 1 provided a self-consistent solution for PISN ejecta, our calculations indicate that this solution is not unique, and has not ruled out lower-mass ejecta on the core-collapse scale (10$M_\odot$). Moreover, if the line at 5,200 Å is [Fe II], then both our model and the model of ref. 1 predict a dominant [Fe II] 7,155 Å line (at the low temperatures and high iron mass expected in PISN), which is not present in the observed spectra. To estimate the nickel mass needed to

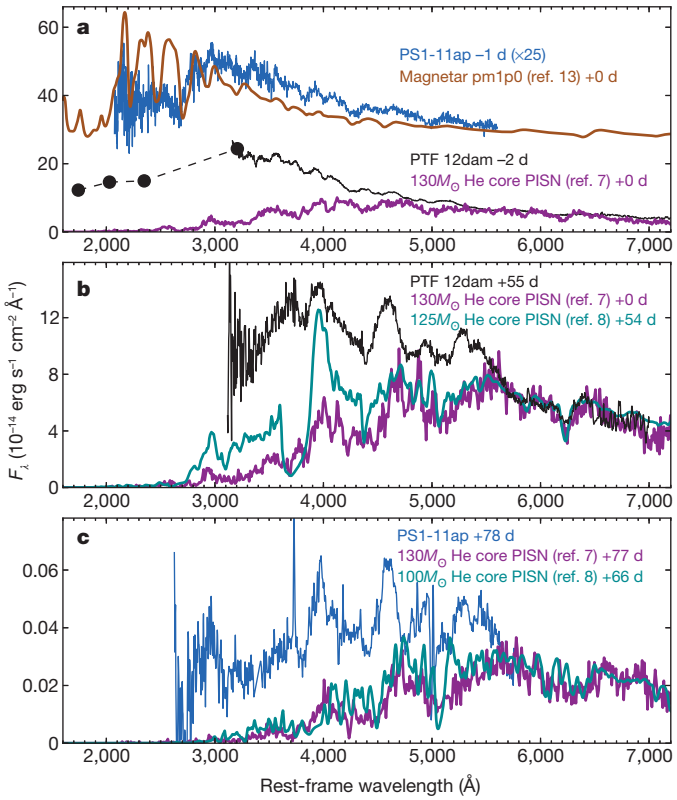

Figure 3 | Spectral comparison with pair-instability and magnetar-driven supernova models. a–c, We compare our ultraviolet and optical data to the predictions of PISN[7,8,13] and magnetar models[13] (lines in models are identified in refs 8 and 13). The absence of narrow lines and hydrogen/helium seems to make interaction-powered colliding-shell models unlikely (for example, the pulsational pair-instability; see Supplementary Information section 5.3). Model spectra are matched to the observed flux in the region 5,500–7,000 Å. **a**, We compare PS1-11ap to a Wolf–Rayet progenitor magnetar model (pm1p0[13]) at peak light (model spectra at later epochs do not currently exist in the literature). The magnetar energy input is equivalent to several solar masses of ^{56}Ni, in ejecta of only 6.94$M_\odot$. The high internal-energy-to-ejecta-mass ratio keeps the ejecta hot and relatively highly ionized, resulting in a blue continuum to match our observations. Moreover, this energy source does not demand the high mass of metals intrinsic to the PISN scenario[7,8]. Redward of the Mg II line at 2,800 Å, this model shows many of the same Fe III and O II lines dominating the observed spectra, although the strengths of the predicted Si III and C III lines in the near-ultraviolet are greater than those observed in PS1-11ap. We also compare PTF 12dam at peak to a 130$M_\odot$ He core PISN model[7]. The model spectrum has intrinsically red colours below 5,000 Å owing to many overlapping lines from the large mass of iron-group elements and intermediate-mass elements. Our rest-frame ultraviolet spectra of PS1-11ap, and ultraviolet photometry of PTF 12dam, show that the expected line blanketing/absorption is not observed. **b**, PTF 12dam compared to models of 125–130$M_\odot$ PISNs[7,8] at 55 days. Although the observed spectrum has cooled, the models still greatly under-predict the flux blueward of 5,000 Å. **c**, PS1-11ap, at 78 days, compared to 100–130$M_\odot$ PISN models[7,8] at similar epochs. Again, our observations are much bluer than PISN models. In particular, PS1-11ap probes the flux below 3,000 Å, where we see the greatest discrepancy.

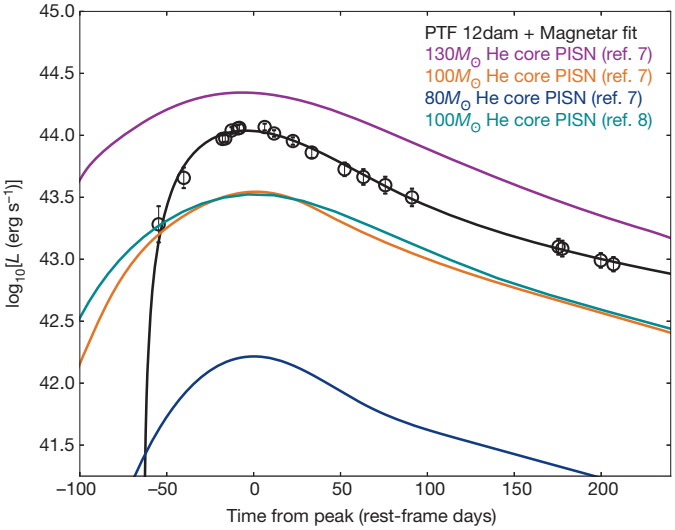

Figure 4 | Bolometric light curve and magnetar fit. Our PTF 12dam bolometric light curve (open circles), comprising Swift observations in the near-ultraviolet, extensive *griz* imaging, and multi-epoch near-infrared (*JHK*) data (Supplementary Information section 5), is well fitted by our semi-analytic magnetar model[21] (black line) (see Supplementary Information section 5.4). This model, with magnetic field $B \approx 10^{14}$ G and spin period $P \approx 2.6$ ms, can fit both the rise and decay times of the light curve. A large ejecta mass of ~10–16$M_\odot$ is required—significantly higher than typically found for type Ibc supernovae[28], but similar to the highest estimates for SN 2011bm[29] and SN 2003lw[30] (though well below the >80$M_\odot$ expected in PISNs). In the context of the magnetar model, the parameters of our fit are consistent with the observed spectroscopic relation to super-luminous supernovae of type I. Fits to a sample of such objects using the same model[21] found uniformly lower ejected masses and higher magnetic fields than in PTF 12dam. The large ejecta mass here results in a slow light-curve rise and broad peak compared to other super-luminous supernovae of type Ic[2,3,21], and would explain the slower spectroscopic evolution, including why the spectrum is not fully nebular at 200 days. The weaker B field means that the magnetar radiates away its rotational energy less rapidly, so that more of the heating takes place at later times; this gives the impression of a radioactive tail. Higher ejected mass and weaker magnetar wind may account for the lower velocities in slowly declining events. Also shown for comparison are bolometric light curves of model PISNs[7,8] from 80–130$M_\odot$ He cores (coloured lines). Although PISNs from less massive progenitors do show faster rise times, the rise of PTF 12dam is too steep to be consistent with the PISN explosion of a He core that is sufficiently massive to generate its observed luminosity. Errors bars, $\pm 1\sigma$ photometry, combined in quadrature.

power PTF 12dam radioactively, we constructed a bolometric light curve from our near-ultraviolet to near-infrared photometry (Fig. 4). PTF 12dam is brighter than SN 2007bi, and fitting it with radioactively powered diffusion models[18,20] requires ~15$M_\odot$ of ^{56}Ni in ~15–50$M_\odot$ of ejecta — combinations that are not produced in any physical model (Extended Data Fig. 6; Supplementary Information section 5.1). Furthermore, such large nickel fractions are clearly not supported by our spectra.

The combination of relatively fast rises and blue spectra, lacking ultraviolet line blanketing, shows that PTF 12dam, PS1-11ap and probably SN 2007bi are not pair-instability explosions. We suggest here one model that can consistently explain the data. A magnetar-powered supernova can produce a light curve with the observed rise and decline rates as the neutron star spins down and reheats the ejecta[13,14,16,17]. It has been suggested that ~10% of core-collapses may form magnetars[14]. Although their initial-spin distribution is unknown, periods $\gtrsim$ 1 ms are physically plausible. This mechanism has already been proposed for SN 2007bi[14], as well as for fast-declining superluminous type-I supernovae[2,21]. We fitted a magnetar-powered diffusion model[21,22] to the bolometric light curve of PTF 12dam (Fig. 4), and found a good fit for magnetic field $B \approx 10^{14}$ G and spin period $P \approx 2.6$ ms, with an ejecta mass of ~10–16$M_\odot$. At peak, the r-band luminosities of PTF 12dam and PS1-11ap are ~1.5 times that of SN 2007bi. Scaling our light curve by this factor, our model implies a similar ejected mass for SN 2007bi, with a slower-spinning magnetar ($P \approx 3.3$ ms), comparable to previous models[14]. If the magnetar theory is correct for normal superluminous type-I supernovae[2,21], our objects could be explained as a subset in which larger ejected masses and weaker magnetic fields result in slower photometric and spectroscopic evolution.

This leaves no unambiguous PISN candidates within redshift $z < 2$ (although possible examples exist at higher redshift[4]). We used the properties of the Pan-STARRS1 Medium Deep Survey (PS1 MDS, with a nightly detection limit of ~23.5 mag in g,r,i-like filters[21,23,24]) to constrain

the local rate of stripped-envelope PISNs. We simulated PS1 MDS observations of 80, 100 and 130$M_\odot$ helium core PISN models[7] using our own Monte Carlo code[25] (Supplementary Information section 6), requiring an apparent magnitude <21 in at least one bandpass and a continuous 100-day (observer-frame) window of PS1 monitoring before considering an event a candidate PISN detection. Initially assuming a rate of 10^{-5} $R_{\rm CCSN}$ (where $R_{\rm CCSN}$ is the rate of occurrence of core-collapse supernovae[26]) for each model, we typically find five 100$M_\odot$ PISN candidates per year, at $z < 0.6$. The 130$M_\odot$ explosions have peak near-ultraviolet magnitudes of -22, resulting in apparent $r_{\rm P1}$ and $i_{\rm P1}$ magnitudes <20. PS1 should detect $>90\%$ of these within $z < 0.6$ (ten or more per year). Taking the 100$M_\odot$ result, the fact that we have not detected a single transient with these properties in the three years of PS1 is inconsistent with our assumed explosion rate at a level of 3.9σ (Poisson statistics). This implies a 3σ upper limit on their rate (within $z < 0.6$) of $<6 \times 10^{-6}$ $R_{\rm CCSN}$; even allowing another factor of $\sim$2 to conservatively cover detection issues such as bad pixels or bright nearby stars, the rate of occurrence of super-luminous PISNs of type Ic must be at least a factor of ten lower than the overall rate of type-I superluminous supernovae[12]. PS1-11ap was our best candidate for a PISN explosion, but it fails to match the models. However, our calculation suggests that almost all the lower-mass (80$M_\odot$) PISNs would escape detection. Future searches for PISN candidates should target these fainter explosions at lower redshift (and larger volumes), or the more luminous candidates at $z > 1$.

We conclude that the classification of some slow-fading super-luminous supernovae[12] as radioactively driven is not supported observationally, and propose that these events can be united with virtually all known type-Ic super-luminous supernovae into a single class. Magnetar-powered models can explain their brightness and colours, and account for their diversity. The low upper limit we find for the rate of very massive PISNs reduces their potential impact on cosmic chemical evolution within $z \lesssim 1$. This relieves possible tension between their proposed existence in the nearby Universe, and the lack of detected chemical enrichment signatures in metal-poor stars and damped Lyman-α systems[27].

Online Content Any additional Methods, Extended Data display items and Source Data are available in the online version of the paper; references unique to these sections appear only in the online paper.

Received 10 May; accepted 9 August 2013.

1. Gal-Yam, A. *et al.* Supernova 2007bi as a pair-instability explosion. *Nature* **462,** 624–627 (2009).
2. Quimby, R. M. *et al.* Hydrogen-poor super-luminous stellar explosions. *Nature* **474,** 487–489 (2011).
3. Chomiuk, L. *et al.* Pan-STARRS1 discovery of two ultraluminous supernovae at z~0.9. *Astrophys. J.* **743,** 114–132 (2011).
4. Cooke, J. *et al.* Super-luminous supernovae at redshifts of 2.05 and 3.90. *Nature* **491,** 228–231 (2012).
5. Barkat, Z., Rakavy, G. & Sack, N. Dynamics of supernova explosion resulting from pair formation. *Phys. Rev. Lett.* **18,** 379–381 (1967).
6. Rakavy, G. & Shaviv, G. Instabilities in highly evolved stellar models. *Astrophys. J.* **148,** 803–816 (1967).
7. Kasen, D., Woosley, S. E. & Heger, A. Pair instability supernovae: light curves, spectra, and shock breakout. *Astrophys. J.* **734,** 102 (2011).
8. Dessart, L., Waldman, R., Livne, E., Hillier, D. J. & Blondin, S. Radiative properties of pair-instability supernova explosions. *Mon. Not. R. Astron. Soc.* **428,** 3227–3251 (2013).
9. Heger, A. & Woosley, S. E. The nucleosynthetic signature of population III. *Astrophys. J.* **567,** 532–543 (2002).
10. Young, D. R. *et al.* Two type Ic supernovae in low-metallicity, dwarf galaxies: diversity of explosions. *Astron. Astrophys.* **512,** A70 (2010).
11. Pastorello, A. *et al.* Ultra-bright optical transients are linked with type Ic supernovae. *Astrophys. J.* **724,** L16–L21 (2010).
12. Gal-Yam, A. Luminous supernovae. *Science* **337,** 927–932 (2012).
13. Dessart, L., Hillier, D. J., Waldman, R., Livne, E. & Blondin, S. Super-luminous supernovae: ^{56}Ni power versus magnetar radiation. *Mon. Not. R. Astron. Soc.* **426,** L76–L80 (2012).
14. Kasen, D. & Bildsten, L. Supernova light curves powered by young magnetars. *Astrophys. J.* **717,** 245–249 (2010).
15. Quimby, R. M. *et al.* Discovery of a super-luminous supernova, PTF12dam. *Astron. Tel.* **4121** (2012).
16. Thompson, T. A., Chang, P. & Quataert, E. Magnetar spin-down, hyperenergetic supernovae, and gamma-ray bursts. *Astrophys. J.* **611,** 380–393 (2004).
17. Woosley, S. E. Bright supernovae from magnetar birth. *Astrophys. J.* **719,** L204–L207 (2010).
18. Umeda, H. & Nomoto, K. How much ^{56}Ni can be produced in core-collapse supernovae? Evolution and explosion of 30–100M$_\odot$ stars. *Astrophys. J.* **673,** 1014–1022 (2008).
19. Jerkstrand, A., Fransson, C. & Kozma, C. The ^{44}Ti-powered spectrum of SN 1987A. *Astron. Astrophys.* **530,** A45 (2011).
20. Moriya, T. *et al.* A core-collapse model for the extremely luminous type Ic SN2007bi: an alternative to the pair-instability supernova model. *Astrophys. J.* **717,** L83–L86 (2010).
21. Inserra, C. *et al.* Super-luminous Ic supernovae: catching a magnetar by the tail. *Astrophys. J.* **770,** 128 (2013).
22. Arnett, W. D. Type I supernovae. I — Analytic solutions for the early part of the light curve. *Astrophys. J.* **253,** 785–797 (1982).
23. Tonry, J. L. *et al.* First results from Pan-STARRS1: faint, high proper motion white dwarfs in the Medium-Deep fields. *Astrophys. J.* **745,** 42 (2011).
24. Berger, E. *et al.* Ultraluminous supernovae as a new probe of the interstellar medium in distant galaxies. *Astrophys. J.* **755,** L29 (2012).
25. Young, D. R. *et al.* Core-collapse supernovae in low-metallicity environments and future all-sky transient surveys. *Astron. Astrophys.* **489,** 359–375 (2008).
26. Dahlen, T. *et al.* High-redshift supernova rates. *Astrophys. J.* **613,** 189–199 (2004).
27. Kobayashi, C., Tominaga, N. & Nomoto, K. Chemical enrichment in the carbon enhanced damped Lyα system by population III supernovae. *Astrophys. J.* **730,** L14 (2011).
28. Drout, M. R. *et al.* The first systematic study of type Ibc supernova multi-band light curves. *Astrophys. J.* **741,** 97 (2011).
29. Valenti, S. *et al.* A spectroscopically normal type Ic supernova from a very massive progenitor. *Astrophys. J.* **749,** L28 (2012).
30. Mazzali, P. A. *et al.* Models for the type Ic hypernova SN 2003lw associated with GRB 031203. *Astrophys. J.* **645,** 1323 (2006).

Supplementary Information is available in the online version of the paper.

Acknowledgements We thank D. Kasen and L. Dessart for sending us their model data. The Pan-STARRS1 Surveys (PS1) have been made possible through contributions of the Institute for Astronomy, the University of Hawaii, the Pan-STARRS Project Office, the Max Planck Society (and its participating institutes, the Max Planck Institute for Astronomy, Heidelberg, and the Max Planck Institute for Extraterrestrial Physics, Garching), The Johns Hopkins University, Durham University, the University of Edinburgh, Queen's University Belfast, the Harvard-Smithsonian Center for Astrophysics, the Las Cumbres Observatory Global Telescope Network Incorporated, the National Central University of Taiwan, the Space Telescope Science Institute, NASA grant no. NNX08AR22G issued through the Planetary Science Division of the NASA Science Mission Directorate, National Science Foundation grant no. AST-1238877, and the University of Maryland. S.J.S. acknowledges FP7/2007-2013/ERC Grant agreement no. 291222; J.L.T. and R. P. Kirshner acknowledge NSF grants AST-1009749, AST-121196; G.L. acknowledges Swedish Research Council grant no. 623-2011-7117; A.P., L.T., E.C., S.B. and M.T.B. acknowledge PRIN-INAF 2011. Work is based on observations made with the following telescopes: the William Herschel Telescope, Gran Telescopio Canarias, the Nordic Optical Telescope, Telescopio Nazionale Galileo, the Liverpool Telescope, the Gemini Observatory, the Faulkes North Telescope, the Asiago Copernico Telescope and the United Kingdom Infrared Telescope.

Author Contributions M.N. carried out the optical and near-infrared photometric and spectroscopic data analysis and wrote the manuscript. S.J.S. initiated, coordinated and managed the project, and contributed to manuscript preparation. A.J. carried out the theoretical modelling aspects, with contributions from S.A.S. C.I. reduced the ultraviolet data and assisted in all aspects of the analysis, including writing software to determine *k*-corrections and bolometric luminosity and running line identification routines. M.McC. provided the PS1-11ap reduced data. M.F. and R.K. carried out observations and coordinated Liverpool Telescope and Faulkes Telescope data. D.W., T.-W.C., K.S., D.R.Y., S.V., M.T.B., M.F., R.K. and Y.U. worked on finding PS1 transients using manual searching and software development. D.R.Y. wrote and adapted the Monte Carlo code described. F.B. and R. P. Kudritzky provided Gemini data through joint programmes. D.A.H. provided data from Faulkes North Telescope. A.P., L.T., E.C. and S.B. undertook observations with the Asiago telescopes. S.M., E.K., T.K., G.L., J.S. and F.T. provided data and relevant reductions through their Nordic Optical Telescope programmes. E.B., R.C., G.N., R.J.F., A.R., S.R., A.G.R., D.S., S.G., S.R., W.M.W.-V., N.S., R.M., R.L., A.S., D.M. and R. P. Kirshner worked on PS1 data analysis including difference imaging for PS1-11ap through the photpipe software at CfA/JHU and ensuring difference images were photometrically calibrated, and manual searching and spectroscopic follow-up of PS1 transients. N.E.-R., A.M.-G. and S.T. provided and reduced the GTC spectral data. J.L.T., M.E.H., W.S.B., K.C., H.A.F., E.A.M., N.K., N.M., J.M., P.A.P., C.W.S., W.S. and C.W. worked on designing and operating the PS1 system, from hardware through to software and data reduction routines.

Author Information Reprints and permissions information is available at www.nature.com/reprints. The authors declare no competing financial interests. Readers are welcome to comment on the online version of the paper. Correspondence and requests for materials should be addressed to M.N. (mnicholl03@qub.ac.uk).

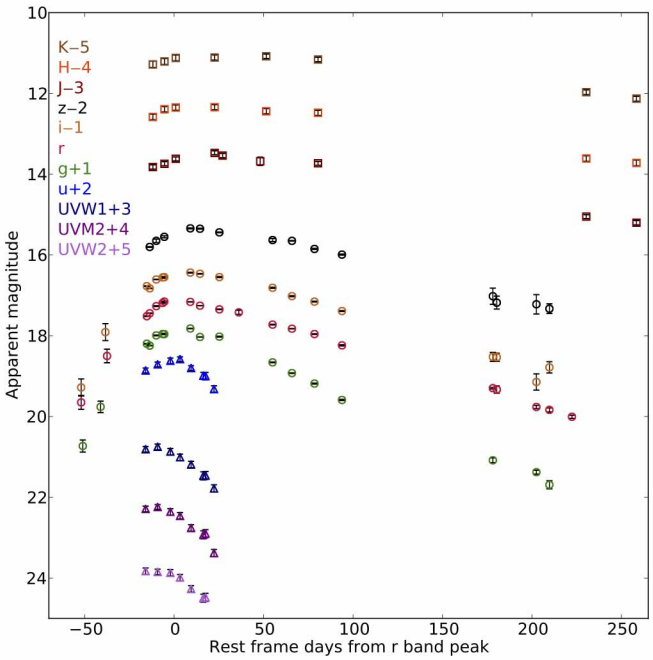

Extended Data Figure 1 | Multi-colour photometry of PTF 12dam. Observed light curve of PTF 12dam in UVW2, UVM2, UVW1, *u*, *g*, *r*, *i*, *z* (AB magnitudes) and *J*, *H*, *K* (Vega magnitude system).

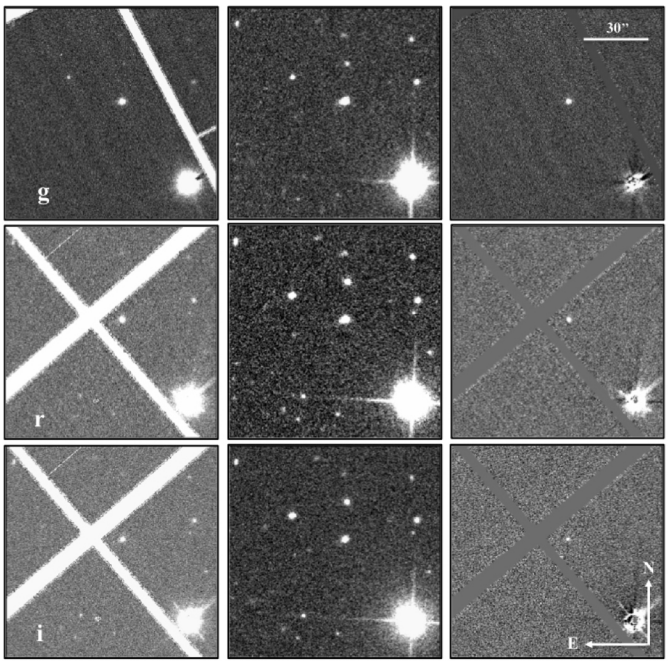

Extended Data Figure 2 | Image subtraction for the three earliest Pan-STARRS1 epochs of PTF 12dam in g_{P1}, r_{P1} and i_{P1}, using SDSS frames as reference images (taken on 11 February 2003). These illustrate reliable image subtraction, resulting in clear detections of PTF 12dam at early phases. The images on the left are our PS1 detections, those in the centre are the SDSS templates, and on the right are the differences between the two. The bright star in the lower right was saturated and hence does not subtract cleanly. At each PS1 epoch there are two images, taken as transient time interval pairs. Photometry was carried out and determined in the SDSS photometric system to match the bulk of the follow-up *griz* imaging. The white areas are gaps between the 590 × 598 pixel cells in the PS1 chip arrays.

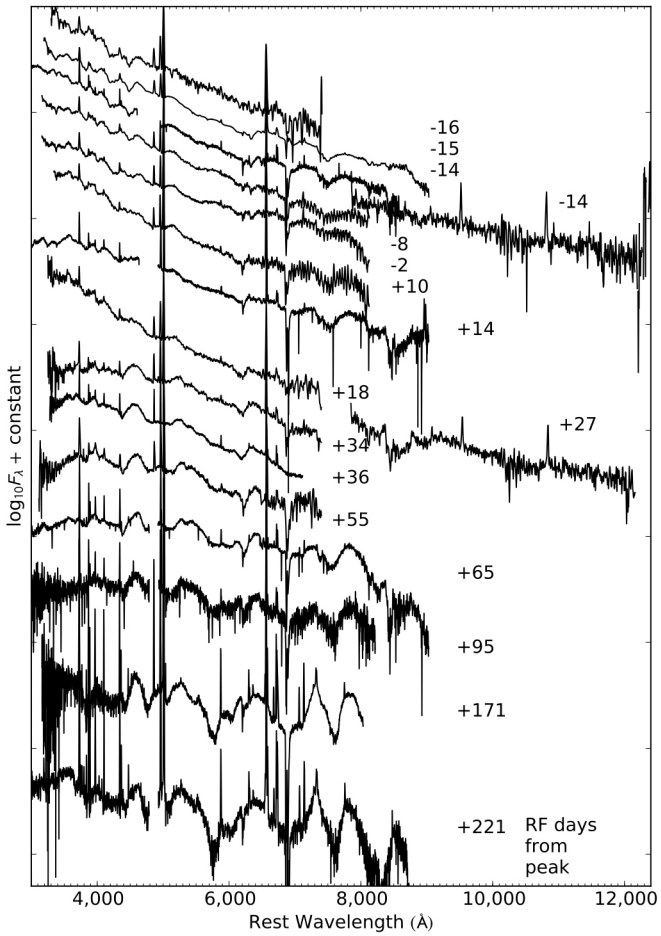

Extended Data Figure 3 | Spectral evolution of PTF 12dam. Full time-series optical and near-infrared spectroscopy of PTF 12dam, from two weeks before maximum light to an extended pseudo-nebular phase at 100 to >200 days afterwards. A Starburst99 model continuum spectral energy distribution for the host galaxy has been calibrated against SDSS and GALEX (Galaxy Evolution Explorer) photometry and subtracted from the last three spectra. RF, rest-frame.

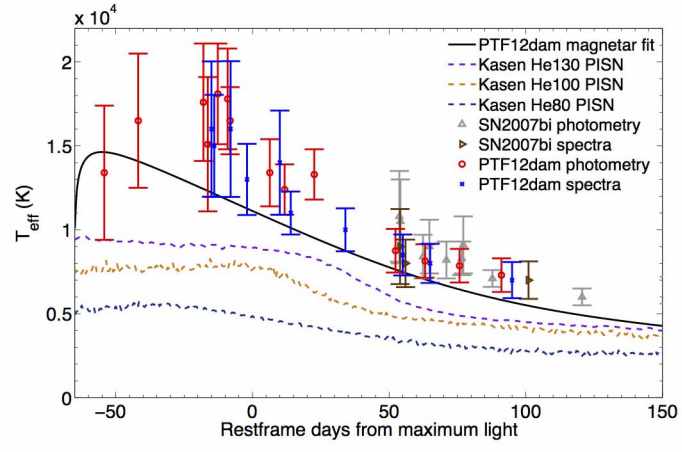

Extended Data Figure 4 | Effective temperature evolution of PTF 12dam and SN 2007bi, compared with magnetar-powered and pair-instability models. The magnetar model comes much closer to reproducing the high photospheric temperatures we observe, and matches the gradient of the decline phase well. PISN models do not reach such high effective temperatures, and show an approximately 100-day temperature plateau as they rise, before declining after maximum light.

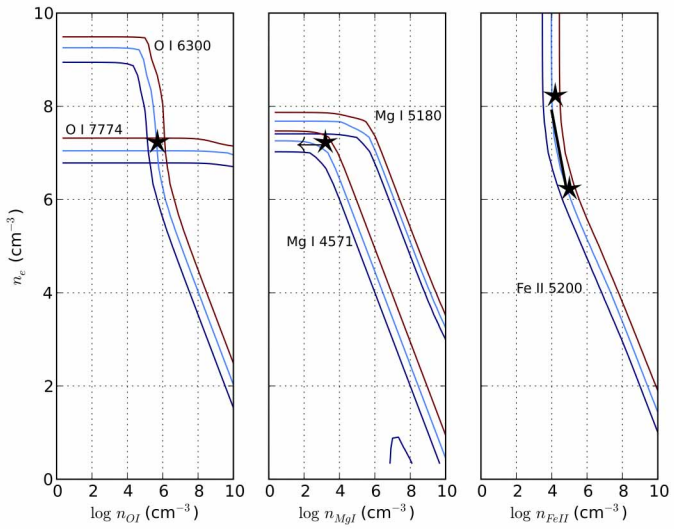

Extended Data Figure 5 | Modelling of the O I, Mg I and Fe II line fluxes in SN 2007bi at 367 days post-peak. We plot contours for oxygen, magnesium and iron line fluxes predicted by our model in units of $L = 10^{40}$ erg s^{-1} (dark blue = $L/3$; light blue = L; red = $3L$; where L is the approximate luminosity of the lines in the 367-day post-peak spectrum of SN 2007bi) as functions of the respective ion density, $\{n_{\mathrm{O\,I}}, n_{\mathrm{Mg\,I}}, n_{\mathrm{Fe\,II}}\}$, and electron density, n_e, at 5,000 K (approximately the temperature derived for the iron zone from the relative strengths of iron lines). The panels for O I and Mg I show two lines (O I 6,300, 7,774 Å; Mg I 4,571, 5,180 Å), whereas Fe II shows only contours for the 5,200 Å blend. No blending is likely to occur for any of the oxygen lines; the region where they intersect therefore gives the allowed densities, constraining n_e to about 10^7 cm^{-3} (this is quite insensitive to the temperature we assume). Blending is also unlikely for Mg I] 4,571 Å, and the allowed Mg I density is therefore the intersection of this contour with $n_e \approx 10^7$ cm^{-3}, which can be seen to give $n_{\mathrm{Mg\,I}} \lesssim 10^3$ cm^{-3}. At this magnesium density, we see that the Mg I 5,180 Å line makes some contribution to the 5,200 Å flux. Also shown is the allowed Fe II density at this temperature, for iron-zone electron densities spanning a factor of ten either side of that in the oxygen/magnesium zones.

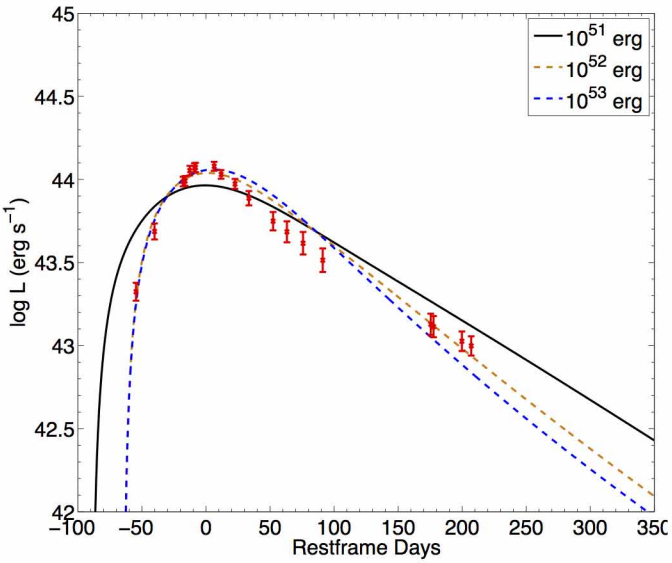

Energy (erg)	Mass of ^{56}Ni ($M_\odot$)	Ejecta Mass ($M_\odot$)	Total rise time (days)	χ^2 / D.O.F.
10^{51}	14.1	14.7	88.9	8.7
10^{52}	14.1	21.5	64.4	1.8
10^{53}	16.1	52.2	64.4	3.0

Extended Data Figure 6 | Fits to the observed bolometric light curve of PTF 12dam with radioactive ^{56}Ni powered ejecta. The formal fits of the models with kinetic energies of 10^{52} and 10^{53} erg are good (see graph), but the required combinations of ^{56}Ni masses and ejecta masses (see data table) are not produced in physical models; such large nickel fractions are only expected to be produced in thermonuclear explosions (supernova Ia or possibly PISN), whereas the total ejected mass corresponds to the core-collapse of a massive star below the pair-instability threshold.

Extended Data Table 1 | Optical photometry of PTF 12dam in SDSS *griz* bands, and *k*-corrections derived from our spectra.

Date	MJD	RF Phase (days)	Telescope	g	K_g	r	K_r	i	K_i	z	K_z
2012-04-13	56030.48	-51.9	PS1			19.45 (0.17)^S	0.20	20.04 (0.21)^S	0.24		
2012-04-14	56031.45	-51.0	PS1	19.62 (0.15)^S	0.11						
2012-04-25	56042.47	-41.1	PS1	18.65 (0.14)^S	0.11						
2012-04-28	56045.48	-38.4	PS1					18.67 (0.21)^S	0.24		
2012-04-29	56046.50	-37.5	PS1			18.30 (0.17)^S	0.20				
2012-05-23	56071.13	-15.2	GTC + OSIRIS	17.09 (0.01)	0.11	17.32 (0.01)	0.20	17.53 (0.01)	0.24		
2012-05-25	56072.92	-13.6	WHT + ACAM	17.13 (0.01)	0.11	17.26 (0.01)	0.19	17.59 (0.01)	0.24	17.52 (0.01)	0.14
2012-05-29	56076.95	-10.0	LT + RATCam	16.88 (0.01)	0.11	17.11 (0.01)	0.16	17.38 (0.01)	0.23	17.37 (0.04)	0.14
2012-06-02	56080.94	-6.4	LT + RATCam	16.84 (0.01)	0.12	17.05 (0.01)	0.14	17.34 (0.02)	0.22		
2012-06-03	56081.94	-5.5	LT + RATCam	16.84 (0.01)	0.12	17.02 (0.01)	0.13	17.33 (0.01)	0.22	17.27 (0.03)	0.14
2012-06-20	56098.03	9.1	TNG + LRS	16.76 (0.01)	0.06	16.97 (0.01)	0.19	17.24 (0.01)	0.20	17.12 (0.01)	0.11
2012-06-25	56104.02	14.5	WHT + ACAM	17.00 (0.01)	0.03	17.05 (0.01)	0.21	17.28 (0.01)	0.19	17.15 (0.01)	0.10
2012-07-07	56116.01	25.3	NOT+ALFOSC	17.05 (0.01)	-0.03	17.15 (0.01)	0.19	17.37 (0.01)	0.18	17.24 (0.01)	0.10
2012-07-17	56128.03	36.2	GTC + OSIRIS			17.25 (0.05)			0.17		
2012-08-09	56148.93	55.0	NOT+ALFOSC	17.76 (0.01)	-0.10	17.51 (0.01)	0.21	17.66 (0.01)	0.15	17.51 (0.04)	0.07
2012-08-21	56160.92	65.9	WHT + ACAM	17.99 (0.01)	-0.07	17.67 (0.01)	0.16	17.88 (0.01)	0.14	17.53 (0.01)	0.05
2012-09-04	56174.85	78.5	NOT+ALFOSC	18.22 (0.01)	-0.03	17.86 (0.01)	0.10	17.99 (0.01)	0.16	17.75 (0.02)	0.05
2012-09-21	56191.86	93.8	WHT + ACAM	18.58 (0.01)	0.01	18.21 (0.01)	0.03	18.20 (0.01)	0.19	17.95 (0.01)	0.02
2012-12-23	56285.21	178.1	LT + RATCam	19.84 (0.06)^S	0.24	19.27 (0.02)^S	0.03	19.47 (0.11)^S	0.05	19.03 (0.20)^S	0.01
2012-12-25	56287.63	180.3	FTN + FS02			19.30 (0.09)^S	0.03	19.49 (0.01)^S	0.05	19.12 (0.11)^S	0.03
2013-01-19	56312.15	202.5	LT + RATCam	20.14 (0.05)^S	0.24	19.72 (0.04)^S	0.04	20.14 (0.20)^S	0.01	19.23 (0.24)^S	-0.03
2013-01-27	56320.21	209.8	LT + RATCam	20.45 (0.10)^S	0.24	19.79 (0.05)^S	0.04	19.78 (0.14)^S	0.00	19.35 (0.12)^S	-0.02
2013-02-10	56334.17	222.4	LT + RATCam			19.96 (0.04)^S	0.04				
2003-02-11	52681.46		SDSS (host)	19.30 (0.01)		19.15 (0.01)		18.70 (0.01)		19.31 (0.07)	

Magnitudes have been corrected for host galaxy contamination; those labelled with a superscript 'S' were determined after image subtraction with SDSS templates (see Supplementary Information section 2.1).

Extended Data Table 2 | Photometry of PTF 12dam outside the optical range.

Date	MJD	Phase	Telescope	UVW2	UVM2	UVW1	SDSS *u* *	J	H	K
2012-05-22	56070.38	-15.9	Swift+UVOT	18.83 (0.08)	18.29 (0.07)	17.81 (0.07)	16.86 (0.06)			
2012-05-26	56074.89	-11.8	TNG+NICS					16.82 (0.05)	16.58 (0.07)	16.28 (0.08)
2012-05-30	56077.80	-9.2	Swift+UVOT	18.85 (0.07)	18.24 (0.06)	17.75 (0.07)	16.71 (0.06)			
2012-06-03	56082.06	-5.4	TNG+NICS					16.74 (0.05)	16.39 (0.07)	16.21 (0.07)
2012-06-07	56085.69	-2.1	Swift+UVOT	18.87 (0.08)	18.36 (0.08)	17.87 (0.08)	16.62 (0.07)			
2012-06-10	56089.03	0.9	NOT+NOTCam					16.62 (0.05)	16.35 (0.07)	16.12 (0.06)
2012-06-13	56091.67	3.3	Swift+UVOT	18.99 (0.08)	18.46 (0.08)	18.01 (0.08)	16.58 (0.06)			
2012-06-20	56098.52	9.5	Swift+UVOT	19.27 (0.08)	18.76 (0.08)	18.19 (0.08)	16.80 (0.06)			
2012-06-27	56106.06	16.3	Swift+UVOT	19.50 (0.10)	18.93 (0.10)	18.47 (0.10)	16.99 (0.08)			
2012-06-28	56107.44	17.6	Swift+UVOT	19.48 (0.10)	18.90 (0.10)	18.46 (0.10)	17.00 (0.09)			
2012-07-04	56112.68	22.3	Swift+UVOT	20.16 (0.09)	19.38 (0.09)	18.78 (0.09)	17.32 (0.08)			
2012-07-04	56113.05	22.6	NOT+NOTCam					16.47 (0.05)	16.34 (0.07)	16.11 (0.06)
2012-07-09	56118.04	27.1	TNG+NICS					16.54 (0.05)		
2012-08-01	56141.25	48.1	UKIRT+WFCAM					16.68 (0.10)		
2012-08-05	56145.03	51.5	NOT+NOTCam						16.44 (0.07)	16.08 (0.06)
2012-09-07	56177.04	80.4	NOT+NOTCam					16.73 (0.05)	16.48 (0.06)	16.16 (0.06)
2013-02-20	56343.00	230.4	NOT+NOTCam					18.05 (0.05)	17.61 (0.07)	16.97 (0.06)
2013-03-22	56374.04	258.4	NOT+NOTCam					18.20 (0.06)	17.72 (0.07)	17.13 (0.06)
2013-04-25	56407.00	288.2	NOT+NOTCam					18.22 (0.07)	17.94 (0.08)	17.25 (0.07)

Ultraviolet photometry in Swift UVOT (Ultraviolet and Optical Telescope) bands, and near-infrared photometry in JHK (for details of the data, see Supplementary Information section 2.1).
* SDSS DR9 host magnitude: $u = 19.67$ (0.03).

Extended Data Table 3 | Pan-STARRS1 photometry of PS1-11ap used in this work.

Date	MJD	Telescope	i_{P1}	z_{P1}
2010-12-31	55561.6	PS1	21.49 (0.02)	
2011-01-09	55570.55	PS1	21.06 (0.02)	
2011-01-15	55576.62	PS1	20.74 (0.02)	
2011-01-22	55583.52	PS1		20.78 (0.04)
2011-01-24	55585.44	PS1	20.47 (0.01)	
2011-01-25	55586.61	PS1		20.70 (0.03)
2011-01-28	55589.56	PS1		20.63 (0.03)
2011-01-31	55592.58	PS1		20.58 (0.04)
2011-02-03	55595.53	PS1		20.54 (0.02)
2011-02-21	55613.44	PS1		20.38 (0.02)
2011-03-11	55631.38	PS1		20.35 (0.03)
2011-03-14	55634.32	PS1		20.41 (0.04)
2011-03-26	55646.43	PS1		20.52 (0.03)
2011-03-29	55649.50	PS1		20.56 (0.06)
2011-04-22	55673.34	PS1		20.73 (0.03)
2011-04-25	55676.34	PS1		20.81 (0.06)
2011-05-01	55682.25	PS1		20.82 (0.04)
2011-05-13	55694.28	PS1		20.90 (0.07)
2011-05-22	55703.28	PS1		20.83 (0.06)
2011-05-25	55706.26	PS1		20.99 (0.07)
2011-05-31	55712.26	PS1		21.02 (0.03)
2011-06-06	55718.26	PS1		21.08 (0.05)
2011-12-30	55925.90	PS1		22.60 (0.14)

The i_{P1} magnitudes are transformed to z_{P1} using the observed colour $i - z = -0.18$ at the earliest z point, MJD = 55583.52, with i linearly interpolated to this epoch (see Supplementary Information section 2.2).

Extended Data Table 4 | Log of spectra for PTF 12dam and the PS1-11ap spectra used in this work.

Date	MJD	RF phase (days)	Instrument	Grism/Grating	Range (Å)	Resolution (Å)
			PS1-11ap			
2011-02-22	55614	-1	WHT + ISIS	R300B; R158R	3150-10500	12
2011-06-22	55734	+78	GN + GMOS	R150	4000-11000	23
			PTF12dam			
2012-05-23	56070.99	-16	Asiago Copernico + AFOSC	Gr04	3400-8200	25
2012-05-24	56071.12	-15	GTC + OSIRIS	R300R	3500-10000	30
2012-05-25	56072.91	-14	WHT + ISIS	R300B; R158R	3250-5100; 5500-9500	3;5
2012-05-26	56073.95	-13	TNG + NICS	IJ	8700-14500	35
2012-06-01	56079.96	-8	NOT + ALFOSC	Gr04	3500-9000	15
2012-06-08	56086.95	-2	NOT + ALFOSC	Gr04	3500-9000	15
2012-06-21	56100.04	+10	NOT + ALFOSC	Gr04	3700-9000	15
2012-06-25	56103.99	+14	WHT + ISIS	R300B; R158R	3200-5200; 5450-10000	6;11
2012-06-29	56107.97	+18	Asiago Copernico + AFOSC	VPH6	3600-10000	15
2012-07-09	56117.99	+27	TNG + NICS	IJ	8700-13500	35
2012-07-17	56125.95	+34	Asiago Copernico + AFOSC	Gr04	3900-8140	13
2012-07-19	56128.03	+36	GTC + OSIRIS	R1000B	3600-7900	7
2012-08-09	56148.95	+55	NOT + ALFOSC	Gr04	3500-8200	20
2012-08-20	56159.92	+65	WHT + ISIS	R300B; R158R	3200-5300; 5450-10000	4;7
2012-09-22	56192.86	+95	WHT + ISIS	R300B; R158R	3200-5300; 5450-10000	6;11
2012-12-16	56277.5	+171	GN + GMOS	B600; R400	3500-8900	3;4
2013-02-10	56334.17	+221	WHT + ISIS	R300B; R158R	3200-5300; 5400-10000	5;10

Spectral evolution of PTF 12dam is plotted in Extended Data Fig. 3. Full PS1-11ap time-series are to be presented elsewhere[31].

31. McCrum, M. *et al.* The super-luminous supernova PS1-11ap: bridging the gap between low and high redshift. *Mon. Not. R. Astron. Soc.* (submitted).